

Methane Storage in Metal–Organic Frameworks: Current Records, Surprise Findings, and Challenges

Yang Peng,^{†,‡} Vaiva Krungleviciute,^{†,‡} Ibrahim Eryazici,[§] Joseph T. Hupp,[§] Omar K. Farha,^{*,§} and Taner Yildirim^{*,†,‡}

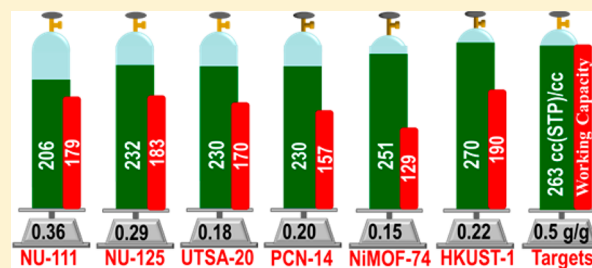
[†]NIST Center for Neutron Research, National Institute of Standards and Technology, Gaithersburg, Maryland 20899-6102, United States

[‡]Department of Materials Science and Engineering, University of Pennsylvania, Philadelphia, Pennsylvania 19104-6272, United States

[§]Department of Chemistry and International Institute for Nanotechnology, Northwestern University, 2145 Sheridan Road, Evanston, Illinois 60208, United States

S Supporting Information

ABSTRACT: We have examined the methane uptake properties of six of the most promising metal organic framework (MOF) materials: PCN-14, UTSA-20, HKUST-1, Ni-MOF-74 (Ni-CPO-27), NU-111, and NU-125. We discovered that HKUST-1, a material that is commercially available in gram scale, exhibits a room-temperature volumetric methane uptake that exceeds any value reported to date. The total uptake is about 230 cc(STP)/cc at 35 bar and 270 cc(STP)/cc at 65 bar, which meets the new volumetric target recently set by the Department of Energy (DOE) if the packing efficiency loss is ignored. We emphasize that MOFs with high surface areas and pore volumes perform better overall. NU-111, for example, reaches ~75% of both the gravimetric and the volumetric targets. We find that values for gravimetric uptake, pore volume, and inverse density of the MOFs we studied scale essentially linearly with surface area. From this linear dependence, we estimate that a MOF with surface area 7500 m²/g and pore volume 3.2 cc/g could reach the current DOE gravimetric target of 0.5 g/g while simultaneously exhibiting around ~200 cc/cc volumetric uptake. We note that while values for volumetric uptake are based on ideal single crystal densities, in reality the packing densities of MOFs are much lower. Finally, we show that compacting HKUST-1 into wafer shapes partially collapses the framework, decreasing both volumetric and gravimetric uptake significantly. Hence, one of the important challenges going forward is to find ways to pack MOFs efficiently without serious damage or to synthesize MOFs that can withstand substantial mechanical pressure.



INTRODUCTION

The demand for alternative fuels is greater now than perhaps ever before due to concerns over national and regional energy security, ground-level air quality, and climate change. While not a renewable fuel, natural gas (NG), comprising chiefly methane, has moved to the forefront as a potential bridging fuel to a low-carbon energy future. Methane delivers roughly twice the energy of coal in terms of the amount of carbon dioxide released. In contrast to coal, methane does so without dissipating mercury or producing uranium- and thorium-rich ash. In the United States, air-quality regulations are driving electricity utilities toward gas-fired power plants as replacements for coal-fired plants. Facilitating the transition has been a spectacular recent drop in the price of natural gas¹ due to deployment of inexpensive technologies for its recovery from shale.

Economic and environmental considerations have also boosted interest in NG as a fuel for transportation, and especially as a replacement for petrol (gasoline). A key challenge is mass- and volume-efficient, ambient-temperature

storage and delivery. One potential solution is to store methane at very high pressures (250 bar) as is done currently by most natural gas powered vehicles today. While suitable for large vehicles such as buses, this solution is less than satisfactory for cars. An alternative solution is to use a porous material to store gas at similarly high density, but substantially lower pressure. Metal–organic frameworks² (MOFs) are nanoporous materials that have great potential for high-density methane storage via physisorption. While utilization of MOFs in methane storage has not received nearly as much attention as utilization for hydrogen storage^{3,4} or capture of carbon dioxide,⁵ a number of researchers have investigated methane uptake⁶ by MOFs. Thus far, several MOFs^{6–13} have been reported to exhibit sizable volumetric capacities for methane uptake at room temperature (see refs 6a and 6r for a recent review of methane storage in MOFs). However, recently the U.S. Department of Energy has initiated a new methane storage program¹⁴ with the following

Received: May 6, 2013

Published: July 10, 2013

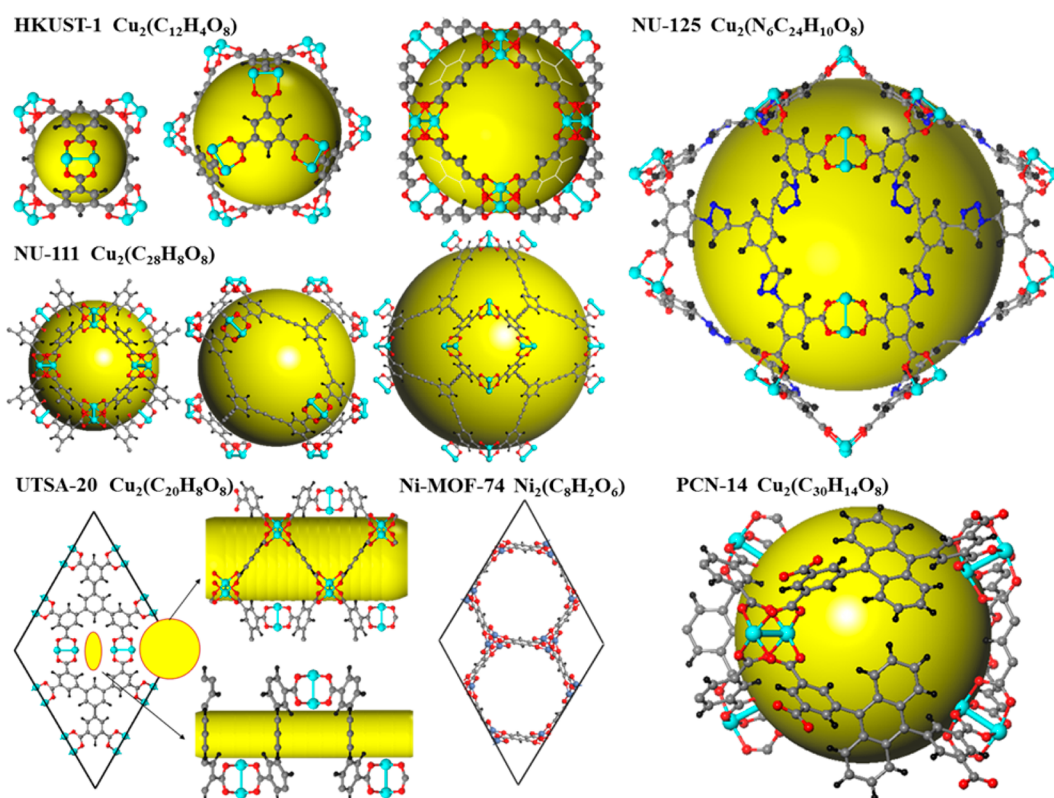


Figure 1. The nanocages and crystal structures of the MOFs under consideration. The empirical formulas for each MOF in desolvated form are also indicated. Some of the atoms are not shown for clarity. The gray, black, red, cyan, and blue spheres represent carbon, hydrogen, oxygen, copper, and nitrogen atoms, respectively.

ambitious targets: 0.5 g (CH_4)/g(sorbent) for gravimetric capacity and $\rho = 0.188 \text{ g/cm}^3$ (11.74 mmol/cc) for minimum required volumetric capacity, which corresponds to the density of compressed natural gas (CNG) at 250 bar and 298 K. The new volumetric target is equivalent to 263 cc (STP: 273.15 K, 1 atm)/cc. If we consider 25% packing loss, the required volumetric target becomes 330 cc(STP)/cc, which is significantly higher than the previous target of 180 cc(STP)/cc at 35 bar.

With these new targets, now is an opportune time to evaluate the most promising existing MOFs at pressures higher than 35 bar (the upper bound of most previous studies) and to assess gravimetric uptake, which has not usually been considered in earlier studies. A typical pipeline pressure is 35 bar, but a more relevant storage pressure is 65 bar, as this corresponds roughly to the upper limit achievable with comparatively inexpensive two-stage compressors. Also important to consider are distinctions between excess uptake, total uptake, and working capacity (deliverable capacity). A representative lower pressure bound for NG delivery to a vehicle engine is 5 bar. Thus, an important design and assessment consideration is how much methane is stored, but stranded, between 0 and 5 bar.

Re-evaluation also provides an opportunity to (a) take advantage of advances in MOF synthesis and activation that may yield larger surface areas and pore volumes than those previously obtained, (b) benchmark experimental surface areas against computationally estimated maximum values, and (c) standardize comparisons to a specific experimental temperature (298 K). Using previously reported results obtained at temperatures lower than 298 K and/or interpreted using densities of nonactivated (i.e., solvated) MOFs, would skew

comparisons, most notably by overestimating volumetric capacities relative to newly measured and analyzed data and materials. Hence, to yield the most consistent and useful experimental benchmarks for studies going forward, it is important to compare data obtained by the same experimentalists and on the same volumetric Sievert apparatus.¹⁵ Herein, we report such a study. Perhaps our most surprising finding is that HKUST-1,⁸ a MOF that is available commercially¹⁶ in gram scale, exhibits the highest total, ambient temperature, volumetric uptake of CH_4 of any MOF reported thus far. The value for HKUST-1 at 65 bar and 298 K (and using the material's single-crystal density) is 267 cc(STP)/cc, on par with a CNG tank at 255 bar.

With these results in mind, we additionally examined how MOF packing density relates to experimentally obtainable volumetric working capacity, and how intentional MOF compaction and wafer formation influence both volumetric and gravimetric working capacities. These considerations are likely to lead to a reordering of MOF performance rankings and underscore the need to move toward materials that are efficiently packable, yet capable of withstanding mechanical compression and retaining full sorption capacity. With the most promising existing MOFs now uniformly experimentally evaluated on an applications-relevant basis, we anticipate that the results of future investigations with new materials and/or processing techniques will be straightforward to compare against these benchmark findings.

EXPERIMENTAL SECTION

We chose to test the six MOFs shown in Figure 1. The first five feature copper(II) paddle-wheel nodes. The last one is a nickel(II) variant of

Table 1. BET Surface Areas, Pore Volumes (Measured by N₂ and CH₄), and Densities, ρ , of the MOFs That Are Studied^a

MOFs	BET (m ² /g)		V _{pore} (cc/g)			ρ (g/cm ³)	metal (mmol/cc)
	N ₂	calcd	N ₂	CH ₄	calcd		
HKUST-1	1850	2064	0.78	0.78	0.78	0.883	4.38
Ni-MOF-74	1350	1240	0.51	0.52	0.49	1.206	7.74
PCN-14	2000	2170	0.85	0.78	0.76	0.829	2.59
UTSA-20	1620	1960	0.66	0.66	0.69	0.909	3.61
NU-125	3120	3680	1.29	1.23	1.32	0.578	1.82
NU-111	4930	4650	2.09	2.12	2.03	0.409	1.36

^aThe last column shows the volumetric metal content in each MOF. The pore volumes and surface areas are calculated (calcd) using PLATON¹⁸ and nonorthoSAs,¹⁹ respectively. The pore volumes reported in the literature for these MOFs are as follows: HKUST-1, 0.75;^{8f} Ni-MOF-74, 0.44;^{9,10} PCN-14, 0.87;⁷ and UTSA-20, 0.63.¹¹

the open-metal-site material, CPO-27, also often called Ni-MOF-74 or Ni(dobdc)₂.^{9,10} These MOFs were selected because they present high surface areas and a broad range of pore sizes, and because previous studies indicated exceptionally high values for methane uptake. Recently, we reported the gas uptake characteristics of NU-111^{13,17} and NU-125.¹² Consequently, here we include only their room-temperature isotherms. For PCN-14,⁷ HKUST-1,⁸ Ni-MOF-74,⁹ and UTSA-20,¹¹ however, we include the results of new sorption measurements made over a wide range of temperatures. In addition to yielding heats of adsorption for methane, at the lowest temperature examined these measurements provide an independent experimental estimate of the maximum amount of methane that can be taken up by a given MOF. MOF samples were freshly prepared using methods reported in the literature (see the Supporting Information for details).^{7–11} All samples were synthesized in several 100 mg quantities. For HKUST-1, PCN-14, and NU-125, we have also repeated the room-temperature isotherm measurements using 1 g samples.

All samples were thoroughly outgassed to remove residue solvent; sample handling was done in a helium-filled glovebox. The samples were activated immediately before sorption measurements. Gas sorption measurements were performed on a carefully calibrated, high accuracy, Sieverts apparatus under computer control. Instrument and measurement-protocol details have been published elsewhere;¹⁵ more details are given in the Supporting Information. All gases were of Research or Scientific grade, with a minimum purity of 99.999%.

RESULTS AND DISCUSSION

Shown in Figure 1 are HKUST-1,⁸ PCN-14,⁷ UTSA-20,¹¹ NU-111,^{13,17} NU-125,¹² and Ni-MOF-74.^{9,10} HKUST-1 has a structure with small cages of ~ 4 , 10, and 11 Å diameter. PCN-14 contains two types of pores: one a relatively small spherical cage of ~ 7 Å, and the other an elliptical cage extending along the *c*-axis. In UTSA-20, two types of one-dimensional channels exist, each presenting unsaturated metal centers to potential guest molecules. One type comprises rectangular pores of about 3.4×4.8 Å, while the second comprises cylindrical pores of ca. 8.5 Å diameter. NU-125 and NU-111 are representative of second-generation MOFs having surface areas exceeding 3000 m²/g. NU-125 has an rht topology with four distinct cages of approximately 24, 16, 15, and 11 Å diameter. NU-111¹⁷ features a face-centered cubic (fcc) structure, with cages located at the origin, tetrahedral, and octahedral sites of an fcc lattice. Ni-MOF-74 consists of a hexagonal array of 1D hexagonal channels of 13.6 Å maximum diameter. The metal nodes form stripes down the length of the channels, with each node connecting three channels.

First, we studied the permanent porosity of the activated MOFs by N₂ adsorption measurements at 77 K (see Figures S8–S12). The BET surface areas, pore volumes, densities of the desolvated structures, and the volumetric metal concentrations are summarized in Table 1. The calculated values utilizing

PLATON¹⁸ are listed as well. The calculated values are in excellent agreement with our measured values. The pore volumes and surface areas reported in Table 1 are mainly consistent with the values reported in the literature. The pore volume of our HKUST-1 sample is 0.78 cc/g, which is 4% higher than the previously report value of 0.75 cc/g.^{8f} The synthesis of HKUST-1 has been improved significantly as evident from increasing pore volumes reported in the literature: 0.33 cc/g by Chui,^{8a} 0.4 cc/g by Lee,^{8d} 0.68 cc/g by Morris,^{8e} and 0.75 cc/g by Rowsell.^{8f} The original synthesis of HKUST-1 used DMF and yielded some cupric oxide as a contaminant, while the new synthesis uses water/ethanol and a small amount of DMF, which is removable via thermal activation.

Next, we studied methane uptake over a wide range of pressures and temperatures as shown in Figure 2. (See Figures S15–S25 for the excess and other isotherms.) The isotherms at 125 K were collected up to the saturation pressure of methane, which is about 2.45 bar. For clarity, we have scaled the pressure axis by 10 for isotherms at this temperature in Figure 2. From the saturation values of the excess isotherms at 125 K, we extracted the pore volumes listed in Table 1. In most of the cases, the pore volumes from nitrogen and methane are in excellent agreement, justifying the use of nitrogen pore volume in calculating the total methane uptake. Interestingly for PCN-14, we observed the largest deviation in pore volume from nitrogen (0.85 cc/g) and methane (0.78 cc/g). The pore volume for PCN-14 was originally reported⁷ as 0.87 cc/g, which is considerably greater than the PLATON-calculated value of 0.76. Similarly, in the original report, the saturation methane uptake at 125 K was reported as 444 cc/cc, which gives a pore volume of 0.94 cc/g. Our saturation value at 125 K is around 355 cc/cc, which gives a pore volume 0.77 cc/g, in excellent agreement with the calculation but somewhat less than the nitrogen pore volume of 0.85 cc/g. This suggests either that methane cannot access all the pores that nitrogen reaches or that there are structural changes with gas loading, yielding different pore volumes with different gases. It would be interesting to perform in situ X-ray/neutron diffraction studies to search for potential structural changes with gas loading. Finally, it is worth mentioning, in calculating the total methane uptake values, we used the pore volumes obtained from nitrogen gas, as is usually done in the literature. However, the small differences in CH₄ and N₂ pore volumes do not create noticeable error in values for total methane uptake, as most of the gas adsorption is due to excess uptake.

The most surprising finding in our study is the exceptionally high volumetric uptake by HKUST-1 as shown in Figure 2. At 35 bar, HKUST-1 exhibits a total CH₄ uptake of 227 cc(STP)/cc, a value midway between the old and new targets. However,

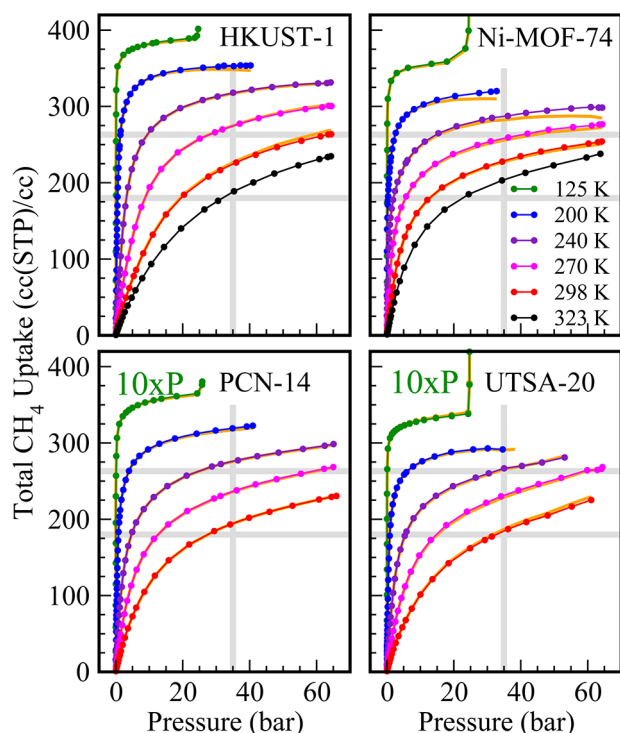


Figure 2. Total volumetric uptake isotherms at various temperatures for HKUST-1, PCN-14, UTSA-20, and Ni-MOF-74. The gray horizontal lines indicate the DOE's old and new volumetric targets, respectively. The pressure axes for the 125 K isotherms are scaled by 10 for clarity. The pore volumes obtained from the saturation uptake at 125 K are summarized in Table 1. The orange lines in the background are isotherms obtained using He-cold volumes with sample, while the other lines are isotherms obtained using cold-volumes of empty cell measured separately (see the Supporting Information for details). Ni-MOF-74 shows significant He-adsorption at high pressures at 240 K and below. The temperature-dependent isotherms for NU-125 and NU-111 are provided in Figures S19,S20 in the Supporting Information (and were recently published in refs 12 and 13).

near 65 bar the total volumetric uptake by HKUST-1 is 267 cc(STP)/cc, slightly higher than the new target, and on par with compressed natural gas tank (CNG) at 255 bar. Hence, having HKUST-1 in the storage tank will effectively reduce the pressure 4-fold, simplifying and reducing the cost associated with the high-pressure technology. It is quite interesting that even though HKUST-1 is one of the earliest MOFs to have been extensively studied,⁸ its exceptionally high volumetric methane uptake properties were missed. In fact, a few years ago, we measured the methane uptake of HKUST-1, which showed low mmol/g uptake;²⁰ we did not recognize, however, its high volumetric uptake.

Because the results of HKUST-1 were quite unexpected, we sought to confirm them and, in particular, to eliminate any possible measurement error attributable to sample size. Thus, we repeated the measurement of room temperature isotherms using 1 g samples of HKUST-1 and NU-125.¹² In Figure S21, we show that the isotherms from 100 mg sample and 1 g sample are almost identical, giving confidence that the reported isotherms here are accurate. We also emphasize that we are reporting two isotherms: one obtained from He-cold volumes with sample in and the other from empty-cell cold volumes, which are measured separately. The isotherms are in excellent agreement,²¹ supporting the accuracy of the measurements. We

tested the reproducibility of the HKUST-1 results by synthesizing several samples ranging from 100 mg to 2 g and obtained the same high uptake values within a deviation of 1–3%. Additionally, we examined a commercially offered sample of HKUST-1¹⁶ and obtained results similar to those for our lab-synthesized samples (see Figure S22). The commercial HKUST-1 sample shows about 5% lower uptake at 65 bar than our samples. In view of the presumably large scale of the commercial synthesis of HKUST-1, this outcome is rather impressive and suggests that HKUST-1 may be a good benchmarking compound for methane sorption by other porous compounds.

Ni-MOF-74 (Figure 2) exhibited remarkably high total volumetric uptake, with values at the highest pressures approaching those seen with HKUST-1. The N₂ isotherm of fresh Ni-MOF-74 gave a pore volume of 0.51 cc/g, that is, somewhat higher than the previously reported value of 0.44 cc/g but in good agreement with the value expected on the basis of PLATON analysis of the corresponding single-crystal X-ray structure.^{10a} Similarly, the absolute methane uptake of 228 cc/cc at 298 K and 35 bar is higher than the previously reported value of 200 cc/cc. Given the differences, we carefully characterized samples from multiple independent syntheses and in every instance obtained larger pore volumes and larger values for methane uptake than previously reported (see Figure S24).

As was pointed out in ref 9, the most exceptional compositional feature of M-MOF-74 (M = Ni, Mg, etc.) is that it has a very high volumetric density of metal centers (see Table 1). Hence, by adsorbing one methane molecule at each metal site, the volumetric uptake reaches 173 cc/cc (3/4 of the total uptake at 35 bar and 298 K). The downside of Ni-MOF-74 is its high density, and therefore the gravimetric uptake is low. Additionally, relying heavily on open metal sites may prove problematic due to competition from water for these sites.²²

The third best value for volumetric uptake comes from PCN-14. At 35 bar and 298 K, and employing the density of the fully activated structure, we obtain 195 cc(STP)/cc at 298 K. We tested the reproducibility of the PCN-14 results by synthesizing several samples ranging from 250 mg to 1 g and obtained the same isotherms within 1% (see Figure S24). The originally reported value of 230 cc(STP)/cc was measured at 290 K, and the density of the structure with coordinated water was used. Hence, our measurements agree reasonably well with earlier findings and clearly support the earlier claim of exceptionally high volumetric uptake of PCN-14 near room temperature.

Finally, UTSA-20 comes as the fourth best MOF in terms of total volumetric uptake. Our measured value of 184 cc(STP)/cc at 35 bar and 298 K is slightly lower than the originally reported value of 195 cc(STP)/cc.

To gain better insight into the nature of the adsorption sites and CH₄–MOF interactions, we extracted isosteric heats of adsorption (Q_{st}) from the temperature-dependent isotherms shown in Figure 2 using the Clausius–Clapeyron equation (see Figures S27–S33). The results are summarized in Figure 3. The initial values of Q_{st} are roughly proportional to the metal content in each MOF (see Table 1), suggesting that the metal center is the initial adsorption site. Ni-MOF-74 shows almost constant Q_{st} and then drops sharply near a loading of one methane molecule per Ni-site. With increasing gas loading, the CH₄–CH₄ interaction starts to play an important role, causing an increase in Q_{st} at high loading. We also note that the Q_{st} at zero coverage limit decreases in MOFs with larger pore volume and surface area. This suggests that the observed initial Q_{st}

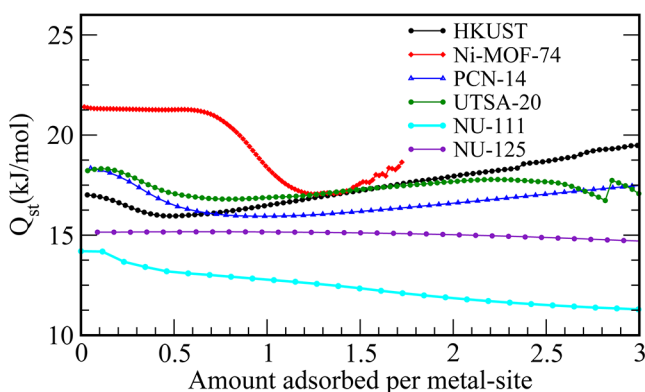


Figure 3. The isosteric heat of adsorptions as a function of methane uptake per metal site for each MOF studied.

values for copper-paddle wheel MOFs are not purely gas-Cu interaction, but there is significant contribution from pore confinement. As the MOF pores get larger as in the case of NU-125 and NU-111, the initial Q_{st} values are very low and represent mainly the copper- CH_4 interaction. We also note that high Q_{st} results in a rapid increase in the isotherm, yielding lower working capacity. Finally, the values of Q_{st} reported in Table 1 are in good agreement with other studies.^{6a,i,s} The biggest discrepancy is the initial Q_{st} for PCN-14 that was reported as 30 kJ/mol, while we obtain a number around 19 kJ/mol.

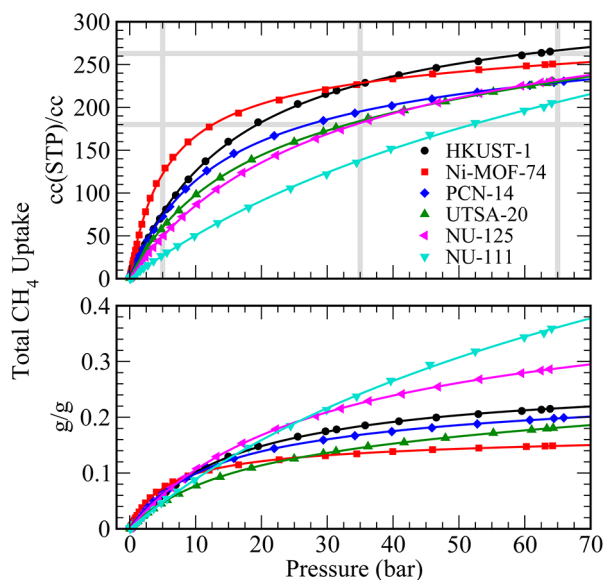


Figure 4. Total volumetric and gravimetric uptakes for six MOFs studied. The gray horizontal lines show the old and new DOE targets for volumetric methane storage. The gravimetric target is 0.5 g of methane per gram of sorbent.

In Figure 4 and Table 2, we compare the room-temperature values for total volumetric (top) and gravimetric (bottom) methane uptake for the six MOFs investigated. From the figure, if the volumetric uptake is the main target, then clearly HKUST-1 and Ni-MOF74 are the top two materials. They both exhibit rather high total uptake, around 230 cc/cc at 35 bar and 250–270 cc/cc at 65 bar, meeting DOE's new volumetric target (if the packing loss is ignored). However, we

note that, in addition to volumetric uptake, the gravimetric uptake is important, and in fact DOE's new target of 0.5 g/g is challenging to reach as shown in the bottom panel of Figure 4. In terms of gravimetric uptake, NU-111, a MOF with a surface area of 4930 m^2/g and a pore volume of 2.09 cc/g, exhibits the best result, reaching almost 75% of both the volumetric and the gravimetric targets. The next best MOF is NU-125, which can be easily synthesized in gram scale.¹²

We note that the total volumetric and gravimetric uptake values are not what determine a material's performance. Ultimately, the working capacity, defined here as the difference in uptake at two pressures (taken as 65 and 5 bar), determines how far a car powered by methane could go. From Table 2, one can conclude that Ni-MOF-74, despite its high total capacity, has a comparatively poor working capacity, indeed, by far the lowest of the six (admittedly high-performing) MOFs examined. The problem with the Ni-containing MOF is that nearly one-half the total capacity at 65 bar is already reached at 5 bar, leaving a comparatively small difference between the two. MOFs presenting fewer open metal sites and engaging in weaker interactions with methane are the better choice for achieving high working capacities. NU-111 and NU-125 fall at the opposite end of the range of MOF densities and metal content, and so should (and do) exhibit better working capacities than Ni-MOF-74. Indeed, the working capacities of these MOFs are comparable to HKUST-1 and PCN-14 even though values for total volumetric uptake by NU-125 and NU-111 are not as high. Interestingly, HKUST-1 seems to be rather optimum for both the total uptake and the working capacity. It shows an impressive 190 cc/cc working capacity, roughly 5% greater than NU-125 and NU-111. However, the mass per unit volume of HKUST-1 is twice that for NU-111. For on-board applications, therefore, NU-111 might well prove superior because it does well in terms of both gravimetric and volumetric capacities. Working capacities can be also optimized by combining temperature and pressure swing processes. For example, if the end point is taken at 323 K (instead of 298 K) and 5 bar, the working capacities of HKUST-1 and Ni-MOF-74 become 216 and 165 cc/cc, respectively.

Next, we address the question of whether there is a MOF that can meet the DOE's new gravimetric target of 0.5 g/g. A simplistic way of addressing this issue is by looking at the correlation between gas uptake values of the MOFs examined here and their surface areas. As shown in Figure 5, these materials (admittedly a small number) show a good linear correlation between the gravimetric uptake and BET surface area. This is somewhat surprising because the total uptake has two contributions. One is from the excess uptake, which should increase roughly linearly with increasing surface area. For the materials studied, this contribution accounts for between 71% and 79% of the total uptake at 65 bar. The second contribution is from the methane that is present solely because of encapsulation by the material's pores. This contribution is estimated as $\rho(\text{CH}_4, P, T) \times V_{\text{pore}}$. The linear dependence of the total uptake therefore suggests that V_{pore} is also roughly linearly proportional to the surface area. Indeed, as shown in Figure 5, this is the case for the MOFs that we have studied here. We obtain a nearly perfectly linear variation of V_{pore} with BET surface area, with the best-fit line passing through the origin (i.e., no surface area \rightarrow no pore volume). From this plot, we estimate that a MOF surface area of about 7500 m^2/g would be needed to reach 0.5 g/g uptake of methane. Among existing MOFs, NU-109 and NU-110 at ca. 7000 and 7100 m^2/g ,

Table 2. Methane Uptake Characteristics of the MOFs under Consideration at 298 K^a

	excess (35 bar)		total (35 bar)		excess (65 bar)		total (65 bar)		density	working capacity		Q _{st} kJ/mol
	g/g	cc/cc	g/g	cc/cc	g/g	cc/cc	g/g	cc/cc		g/g	cc/cc	
DOE target			0.5	263			0.5	263	0.188			
HKUST-1	0.165	204	0.184	227	0.178	220	0.216	267	0.191	0.154	190 ^b	17.0
Ni-MOF-74	0.122	206	0.135	228	0.125	210	0.148	251	0.180	0.077	129 ^b	21.4
PCN-14	0.146	171	0.169	195	0.157	183	0.197	230	0.164	0.136	157	18.7
UTSA-20	0.131	167	0.145	184	0.150	191	0.181	230	0.164	0.134	170	18.2
NU-125	0.192	155	0.225	182	0.223	181	0.287	232	0.166	0.227	183	15.1
NU-111	0.191	109	0.241	138	0.262	150	0.360	206	0.147	0.313	179	14.2

^aThe working capacity is defined as the difference in total uptake between 65 and 5 bar. The density is given in g/cm³ and corresponds to the density of methane gas in a compressed tank, which has the same amount of methane stored in the pores of MOF. ^bThe working capacities are 216 and 165 cc/cc for HKUST-1 and Ni-MOF-74, if the end point is taken at 323 K and 5 bar.

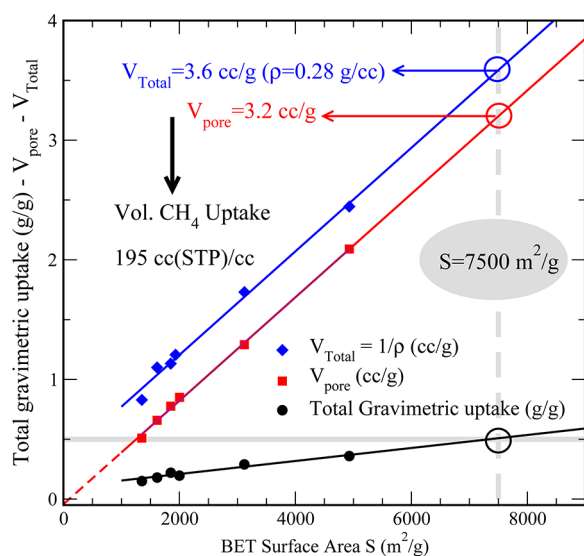


Figure 5. Total gravimetric uptake, pore volume V_{pore} , and total volume V_{Total} ($1/\rho$) as a function of BET surface area, showing a nice linear dependence for each case. The horizontal gray line indicates the DOE's gravimetric target 0.5 g/g, which suggests a MOF with surface area $S = 7500 \text{ m}^2/\text{g}$, pore volume 3.2 g, and density 0.28 g/cm^3 can exhibit 0.5 g/g gravimetric uptake and $\sim 195 \text{ cc/cc}$ volumetric uptake.

respectively, are the two that most closely approaching this benchmark.²³

In Figure 5, we also show that the total volume V_{Total} (i.e., $1/\rho$) is also proportional to surface area. Hence, the $7500 \text{ m}^2/\text{g}$ surface area suggests a density of 0.28 g/cm^3 , which means that our hypothetical MOF with surface area $7500 \text{ m}^2/\text{g}$ and pore volume $V_p = 3.2 \text{ cc/g}$ should exhibit a volumetric uptake of ca. 195 cc/cc .²⁴ The skeletal density ($1/(V_{\text{Total}} - V_{\text{pore}})$) of our extrapolated MOF is 2.5 g/cm^3 , which is less than HKUST-1 (2.8 g/cm^3) and, interestingly, comparable to PCN-14 (2.57 g/cm^3), further giving confidence that such an extrapolated MOF is quite physical and could be within reach experimentally. Needless to say, there are other factors that can affect the gas uptake properties of MOFs, and it is quite possible that we may discover a new MOF that can go beyond the 200 cc(STP)/cc limit that we seem to have from our simple linear correlation shown in Figure 5.

Finally, we address the importance of the density value used in determining the total volumetric uptake. So far, we have used the ideal single-crystal MOF densities to obtain the volumetric uptake values, as this is done traditionally in the literature. However, here we show that the density of a packed

polycrystalline powder sample can differ considerably from the ideal single-crystal density, resulting in experimental volumetric methane capacities that are much lower than we have suggested. In Figure 6, we compare the ideal volumetric

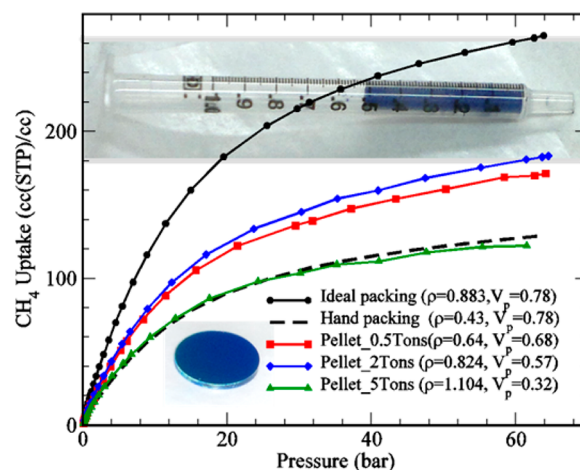


Figure 6. Total volumetric methane uptake by HKUST-1 for different packing densities. The insets show a picture of HKUST-1 powder packed in a 1 mL syringe by hand press (top) and a pressed wafer (bottom).

uptake versus the actual volumetric uptake by an HKUST-1 powder sample packed by hand. As shown in the inset to Figure 6, we filled a 1 mL syringe with MOF powder and pressed hard (by hand) while loading. We could pack about 215 mg into a 0.5 mL volume (Figure 6), yielding a so-called "tapped density" of 0.43 g/cm^3 , that is, roughly one-half of the ideal density of 0.883 g/cm^3 . Hence, the excess volumetric uptake is reduced from its ideal value by one-half. We tried increasing the packing density by pressing the MOFs into wafers as shown in Figure 6. Nitrogen isotherms for the compacted wafer samples show that overall micropore volumes are significantly diminished (see Figure S34). Powder X-ray diffraction measurements are characterized by broadened peaks and reduced intensities gone down significantly, suggesting partial collapse of the HKUST-1 framework with pressure. Indeed, for a sample subjected to 5 tons of mechanical pressure, we obtained a density of 1.1 g/cm^3 , significantly larger than the ideal crystal density of 0.883 g/cm^3 . Even though the density is higher, the total volumetric uptake value is very low as shown in Figure 6 due to loss of the porosity. Clearly needed going forward are either nondestructive ways of compacting high-porosity MOFs,

or alternative MOF formulations and structures that are little affected by mechanical compaction.

CONCLUSIONS

We have synthesized and studied methane uptake by six of the most promising existing MOFs, using a single high-pressure Sievert apparatus and a standardized measurement protocol intended to yield to consistent results. We discovered that both HKUST-1 and Ni-MOF-74 exhibit exceptionally high volumetric methane uptake, with both reaching DOE's new volumetric target at 65 bar if the packing loss is ignored. When working capacities (i.e., deliverable capacities) are examined, however, Ni-MOF-74 fares poorly, as its comparatively high affinity for CH₄ results in substantial uptake between 0 and 5 bar (where 5 bar constitutes the lowest deliverable methane pressure for vehicle applications). Thus, although the targets posed by DOE are for total amounts of methane that can be stored, it is clear that progress at a practical level will require that we and others focus primarily on deliverable capacities.

Because of its ease of synthesis and its commercial availability, we suggest that HKUST-1 would be a good standard methane storage material, with which any new candidate storage material should be compared. When both volumetric and the gravimetric uptake values are considered, we find that second-generation MOFs featuring very large surface areas and pore volumes can perform better overall. For example, NU-111 reaches 75% of DOE's gravimetric and volumetric targets simultaneously (at least if an ideal single-crystal density is assumed). Additionally, this material displays gravimetric and volumetric working capacities (65–5 bar) that are at or near the upper end of the range of values obtained for the six MOFs. For these six, we found that the pore volume, total gravimetric uptake, and the inverse density are all proportional to the BET surface area, suggesting that a hypothetical MOF with $S = 7500 \text{ m}^2/\text{g}$ and $V_{\text{pore}} = 3.2 \text{ cc/g}$ could meet DOE's gravimetric target and at the same time provide volumetric uptake around 200 cc/cc near 65 bar. Finally, we emphasize the importance of determine actual densities and porosities for particulate and potentially compacted MOF samples, if realistic volumetric capacity results are desired. At least for HKUST-1, densities and porosities of compacted samples can differ greatly from those for a fully activated single-crystal, to the detriment, unfortunately, of functional storage capacity. Work that satisfactorily addresses these problems is likely to be critical to develop MOF-based sorbents that can meet DOE's targets for on-board methane storage. We also point out that there are other practical challenges such as cost and chemical stability issues of MOFs that are beyond the scope of this work.

ASSOCIATED CONTENT

Supporting Information

Details of sample synthesis, individual absolute and excess adsorption isotherms, the 77 K N₂ isotherms, consistency and BET plots, and X-ray data of press pellets. This material is available free of charge via the Internet at <http://pubs.acs.org>.

AUTHOR INFORMATION

Corresponding Author

taner@seas.upenn.edu; o-farha@northwestern.edu

Notes

The authors declare no competing financial interest.

ACKNOWLEDGMENTS

T.Y. acknowledges the support by the U.S. Department of Energy through BES Grant No. DE-FG02-08ER46522. O.K.F. and J.T.H. gratefully acknowledge the U.S. DOE's ARPA-E program.

REFERENCES

- (1) In contrast to oil, which is a global commodity, natural gas is a regional commodity, meaning that pricing in North America is largely disconnected from pricing in Asia, Europe, and elsewhere. The disconnect reflects, in part, current restrictions on export of NG from the United States. Pricing is further regionalized by the expense of large-scale trans-oceanic shipment of natural gas. Transport of NG via container ships (as opposed to pipelines) requires that it first be liquefied. Because methane's critical temperature is only 190 K, liquefaction necessarily entails comparatively expensive cooling (to 190 K or below). In practice, gas is usually cooled to about 162 K, thereby allowing for shipping at an internal pressure of 1 bar or less. Liquefaction, ocean transport, and regasification have been estimated to cost about \$3 USD per 1000 cubic feet of gas.
- (2) (a) Ferey, G. *Chem. Soc. Rev.* **2008**, 37, 191. (b) Yaghi, O. M.; O'Keeffe, M.; Ockwig, N. W.; Chae, H. K.; Eddaoudi, M.; Kim, J. *Nature* **2003**, 423, 705. (c) Horike, S.; Shimomura, S.; Kitagawa, S. *Nat. Chem.* **2009**, 1, 695.
- (3) (a) Suh, M. P.; Park, H. J.; Prasad, T. K.; Lim, D.-W. *Chem. Rev.* **2012**, 112, 782. (b) http://www1.eere.energy.gov/hydrogenandfuelcells/storage/current_technology.html.
- (4) (a) Wu, H.; Zhou, W.; Yildirim, T. *J. Am. Chem. Soc.* **2009**, 131, 4995. (b) Dincă, M.; Dailly, A.; Liu, Y.; Brown, C. M.; Neumann, D. A.; Long, J. R. *J. Am. Chem. Soc.* **2006**, 128, 16876. (c) Zhou, W.; Wu, H.; Yildirim, T. *J. Am. Chem. Soc.* **2008**, 130, 15268. (d) Zhou, W.; Yildirim, T. *J. Phys. Chem. C* **2008**, 112, 8132. (e) Wu, H.; Simmons, J. M.; Srinivas, G.; Zhou, W.; Yildirim, T. *J. Phys. Chem. Lett.* **2010**, 1, 1946.
- (5) (a) Sumida, K.; Rogow, D. L.; Mason, J. A.; McDonald, T. M.; Bloch, E. D.; Herm, Z. R.; Bae, T. H.; Long, J. R. *Chem. Rev.* **2012**, 112, 724. (b) Simmons, J. M.; Wu, H.; Zhou, W.; Yildirim, T. *Energy Environ. Sci.* **2011**, 4, 2177. (c) Mason, J. A.; Sumida, K.; Herm, Z. R.; Krishna, R.; Long, J. R. *Energy Environ. Sci.* **2011**, 4, 3030. (d) Wilmer, C. E.; Farha, O. K.; Bae, Y. S.; Hupp, J. T.; Snurr, R. Q. *Energy Environ. Sci.* **2012**, 5, 9849. (e) D'Alessandro, D. M.; Smit, B.; Long, J. R. *Angew. Chem., Int. Ed.* **2010**, 49, 6058. (f) Bae, Y. S.; Snurr, R. Q. *Angew. Chem., Int. Ed.* **2011**, 50, 11586. (g) Liu, Y.; Wang, U. Z.; Zhou, H.-C. *Greenhouse Gases: Sci. Technol.* **2012**, 2, 239. (h) Zhang, Z.; Zhao, Y.; Gong, Q.; Li, Z.; Li, J. *Chem. Commun.* **2013**, 49, 653. (i) Xiang, S.; He, Y.; Zhang, Z.; Wu, H.; Zhou, W.; Krishna, R.; Chen, B. *Nat. Commun.* **2012**, 3, 954. (j) Li, J.-R.; Sculley, J.; Zhou, H.-C. *Chem. Rev.* **2012**, 112, 869.
- (6) (a) Makal, T. A.; Li, J. R.; Lu, W.; Zhou, H.-C. *Chem. Soc. Rev.* **2012**, 41, 7761. (b) He, Y.; Zhou, W.; Krishna, R.; Chen, B. *Chem. Commun.* **2012**, 48, 11813. (c) Wu, H.; Simmons, J. M.; Liu, Y.; Brown, C. M.; Wang, X.-S.; Ma, S.; Peterson, V. K.; Southon, P. D.; Kepert, C. J.; Zhou, H.-C.; Yildirim, Y.; Zhou, W. *Chem.-Eur. J.* **2010**, 16, 5205. (d) Seki, K. *Chem. Commun.* **2001**, 1496. (e) Bourrelly, S.; Llewellyn, P. L.; Serre, C.; Millange, F.; Loiseau, T.; Férey, G. *J. Am. Chem. Soc.* **2005**, 127, 13519. (f) Llewellyn, P. L.; Bourrelly, S.; Serre, C.; Vimont, A.; Daturi, M.; Hamon, L.; Weireld, G. D.; Chang, J.-S.; Hong, D.-Y.; Hwang, Y. K.; Jung, S. H.; Férey, G. *Langmuir* **2008**, 24, 7245. (g) Kim, H.; Samsonenko, D. G.; Das, S.; Kim, G. H.; Lee, H. S.; Dybtsev, D. N.; Berdonosova, E. A.; Kim, K. *Chem. Asian J.* **2009**, 4, 886. (h) Gedrich, K.; Senkovska, I.; Klein, N.; Stoeck, U.; Henschel, A.; Lohe, M. R.; Baburin, I. A.; Mueller, U.; Kaskel, S. *Angew. Chem., Int. Ed.* **2010**, 49, 8489. (i) Klein, N.; Senkovska, I.; Gedrich, K.; Stoeck, U.; Henschel, A.; Mueller, U.; Kaskel, S. *Angew. Chem., Int. Ed.* **2009**, 48, 9954. (j) Klein, N.; Senkovska, I.; Baburin, I. A.; Grüner,

- R.; Stoeck, U.; Schlichtenmayer, M.; Streppel, B.; Mueller, U.; Leoni, S.; Hirscher, M.; Kaskel, S. *Chem.-Eur. J.* **2011**, *17*, 13007. (k) Gr nker, R.; Bon, V.; Heerwig, A.; Klein, N.; M ller, P.; Stoeck, U.; Baburin, I. A.; Mueller, U.; Senkovska, I.; Kaskel, S. *Chem.-Eur. J.* **2012**, *18*, 13299. (l) Stoeck, U.; Krause, S.; Bon, V.; Senkovska, I.; Kaskel, S. *Chem. Commun.* **2012**, 48, 10841. (m) Dietzel, P. D. C.; Besikiotis, V.; Blom, R. J. *Mater. Chem.* **2009**, *19*, 7362. (n) Tan, C.; Yang, S.; Champness, N. R.; Lin, X.; Blake, A. J.; Lewis, W.; Schr der, M. *Chem. Commun.* **2011**, 47, 4487. (o) Park, H. J.; Lim, D.-W.; Yang, W. S.; Oh, T.-R.; Suh, M. P. *Chem.-Eur. J.* **2011**, *17*, 7251. (p) Zhao, X.; Sun, D.; Yuan, S.; Feng, S.; Cao, R.; Yuan, D.; Wang, S.; Dou, J.; Sun, D. *Inorg. Chem.* **2012**, *51*, 10350. (q) Yuan, D.; Zhao, D.; Sun, D.; Zhou, H.-C. *Angew. Chem., Int. Ed.* **2010**, *49*, 5357. (r) Konstas, K.; Osl, T.; Yang, Y.; Batten, M.; Burke, N.; Hill, A. J.; Hill, M. R. *J. Mater. Chem.* **2012**, *22*, 16698. (s) Gallo, M.; Glossman-Mitnik, D. *J. Phys. Chem. C* **2009**, *113*, 6634.
- (7) Ma, S.; Sun, D.; Simmons, J. M.; Collier, C. D.; Yuan, D.; Zhou, H.-C. *J. Am. Chem. Soc.* **2008**, *130*, 1012.
- (8) (a) Chui, S. S. Y.; Lo, S. M. F.; Charmant, J. P. H.; Orpen, A. G.; Williams, I. D. *Science* **1999**, *283*, 1148. (b) Moellmer, J.; Moeller, A.; Dreisbach, F.; Glaeser, R.; Staudt, R. *Microporous Mesoporous Mater.* **2011**, *138*, 140. (c) Jeong, N. C.; Samanta, B.; Lee, C. Y.; Farha, O. K.; Hupp, J. T. *J. Am. Chem. Soc.* **2012**, *134*, 51. (d) Lee, J.-Y.; Li, J.; Jagiello, J. *J. Solid State Chem.* **2005**, *178*, 2527. (e) Xiao, B.; Wheatley, P. S.; Zhao, X.; Fletcher, A. J.; Fox, S.; Rossi, A. G.; Megson, I. L.; Bordiga, S.; Regli, L.; Thomas, K. M.; Morris, R. E. *J. Am. Chem. Soc.* **2007**, *129*, 1203. (f) Rowsell, J. L. C.; Yaghi, O. M. *J. Am. Chem. Soc.* **2006**, *128*, 1304. (g) Senkovska, I.; Kaskel, S. *Microporous Mesoporous Mater.* **2008**, *112*, 108.
- (9) Wu, H.; Zhou, W.; Yildirim, T. *J. Am. Chem. Soc.* **2009**, *131*, 4995.
- (10) (a) Dietzel, P. D. C.; Panella, B.; Hirscher, M.; Blom, R.; Fjellv g, H. *Chem. Commun.* **2006**, 959. (b) Caskey, S. R.; Wong-Foy, A. G.; Matzger, A. J. *J. Am. Chem. Soc.* **2008**, *130*, 10870.
- (11) Guo, Z.; Wu, H.; Srinivas, G.; Zhou, Y.; Xiang, S.; Chen, Z.; Yang, Y.; Zhou, W.; O'Keeffe, M.; Chen, B. *Angew. Chem., Int. Ed.* **2011**, *50*, 3178.
- (12) Wilmer, C. E.; Farha, O. K.; Yildirim, T.; Eryazici, I.; Krungleviciute, V.; Sarjeant, A. A.; Snurr, R. Q.; Hupp, J. T. *Energy Environ. Sci.* **2013**, *6*, 1158. See also: Yan, Y.; Suyetin, M.; Bichoutskaia, E.; Blake, A. J.; Allan, D. R.; Barnett, S. A.; Schroder, M. *Chem. Sci.* **2013**, *4*, 1731.
- (13) Peng, Y.; Srinivas, G.; Wilmer, C. E.; Eryazici, I.; Snurr, R. Q.; Hupp, J. T.; Yildirim, T.; Farha, O. K. *Chem. Commun.* **2013**, 49, 2992.
- (14) See DOE MOVE program at <https://arpa-e-foa.energy.gov/>.
- (15) Sievert: Zhou, W.; Wu, H.; Hartman, M. R.; Yildirim, T. *J. Phys. Chem. C* **2007**, *111*, 16131.
- (16) HKUST-1 commercial available on the website of Sigma-Aldrich: <http://www.sigmaaldrich.com/catalog/product/aldrich/688614?lang=en®ion=US>. Here, we have identified certain commercial suppliers to foster understanding and accurate comparisons to other reported work. Such identification does not imply recommendation or endorsement by us, nor does it imply that the materials or equipment identified are necessarily the best available for the purpose.
- (17) Farha, O. K.; Wilmer, C. E.; Eryazici, I.; Hauser, B. G.; Parilla, P. A.; O'Neill, K.; Sarjeant, A. A.; Nguyen, S. T.; Snurr, R. Q.; Hupp, J. T. *J. Am. Chem. Soc.* **2012**, *134*, 9860.
- (18) PLATON (C) 1980–2011 A. L. Spek, Utrecht University, Padualaan 8, 3584 CH, Utrecht, The Netherlands. The van der Waals radii used in the analysis were C 1.70, H 1.2, Cu 1.4, N 1.5, and O 1.52.
- (19) D ren, T.; Millange, F.; Ferrey, G.; Walton, K. S.; Snurr, R. Q. *J. Phys. Chem. C* **2007**, *111*, 15350.
- (20) To the best of our knowledge, the most detailed methane adsorption measurements on HKUST-1 were done in refs 8b and 8g, both of which were based on gravimetric adsorption measurements. Unlike volumetric adsorption measurements as done in this work, the gravimetric measurements are complicated due to buoyancy effects. The reported excess gravimetric uptake in refs 8b and 8g is around 0.16 g/g, which is 10% lower than our measurement of 0.18 g/g. The difference is probably due to sample quality as the pore volume in ref 8b was 0.71 cc/g, 10% lower than ours, 0.78 cc/g.
- (21) Apart from small deviation due to He-adsorption; see the Supporting Information for a detailed discussion.
- (22) Liu, J.; Benin, A. I.; Furtado, A. M. B.; Jakubczak, P.; Willis, R. R.; LeVan, M. D. *Langmuir* **2012**, *27*, 11451.
- (23) Farha, O. K.; Eryazici, I.; Jeong, N. C.; Hauser, B. G.; Wilmer, C. E.; Sarjeant, A. A.; Snurr, R. Q.; Nguyen, S. T.; Yazaydin, A. O.; Hupp, J. T. *J. Am. Chem. Soc.* **2012**, *134*, 15016.
- (24) Notably, pore volumes for NU-110 (4.40 cm³/g), Bio-MOF-100 (4.30 cm³/g), NU-109 (3.75 cm³/g), and MOF-210 (3.6 cm³/g) already exceed this extrapolated value, implying that a somewhat greater contribution to total uptake from nonspecific pore encapsulation of methane can be expected. See ref 22 and: An, J.; Farha, O. K.; Hupp, J. T. G.; Pohl, E.; Yeh, J. I.; Rosi, N. L. *Nat. Commun.* **2012**, *3*, 604. See also: Furukawa, H.; Ko, N.; Go, Y. B.; Aratani, N.; Choi, S. B.; Choi, E.; Yazaydin, A. O.; Snurr, R. Q.; O'Keeffe, M.; Kim, J.; Yaghi, O. M. *Science* **2010**, *329*, 424.